Journal of Hazardous Materials 470 (2024) 134173

Contents lists available at ScienceDirect

Journal of Hazardous Materials

journal homepage: www.elsevier.com/locate/jhazmat

An analytical strategy for challenging members of the microplastic family: Particles from anti-corrosion coatings

L. Hildebrandt [a], M. Fischer [b], O. Klein [a], T. Zimmermann [a], F. Fensky [a,c], A. Siems [a,d], A. Zonderman [a,e], E. Hengstmann [b], T. Kirchgeorg [b], D. Pröfrock [a,*]

[a] Department for Inorganic Environmental Chemistry, Helmholtz-Zentrum Hereon, Max-Planck-Straße 1, 21502 Geesthacht, Germany
[b] Federal Maritime and Hydrographic Agency (BSH), Marine Sciences Department, Wüstland 2, 22589 Hamburg, Germany
[c] Hochschule für Angewandte Wissenschaften Hamburg, Faculty of Life Sciences, Ulmenliet 20, 20099 Hamburg, Germany
[d] Universität Hamburg, Department of Chemistry, Institute for Inorganic and Applied Chemistry, Martin-Luther-King Platz 6, 20146 Hamburg, Germany
[e] Universität Hamburg, Department of Biology, Marine Ecosystem and Fishery Science, Olbersweg 24, 22767 Hamburg, Germany

HIGHLIGHTS

- Toolbox to study the release and fate of coating particles in the environment.
- Combination of spectroscopic (LDIR, FTIR, Raman) and spectrometric methods (Py-GC/MS, ICP-MS).
- Spectroscopic methods underestimate the abundance of coating particles.
- Py-GC/MS combined with statistical analysis valuable for identification of coatings.
- Multi-elemental analysis identified eco-toxicologically relevant metal(oid)s.

GRAPHICAL ABSTRACT

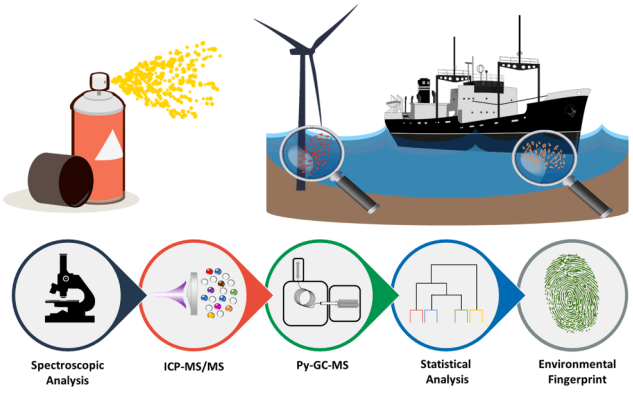

ARTICLE INFO

Keywords:
Paint particles
Spectroscopy
Multivariate statistics
Polymers
Chemometrics

ABSTRACT

Potentially hazardous particles from paints and functional coatings are an overlooked fraction of microplastic (MP) pollution since their accurate identification and quantification in environmental samples remains difficult. We have applied the most relevant techniques from the field of microplastic analysis for their suitability to chemically characterize anti-corrosion coatings containing a variety of polymer binders (LDIR, Raman and FTIR spectroscopy, Py-GC/MS) and inorganic additives (ICP-MS/MS). We present the basis of a possible toolbox to study the release and fate of coating particles in the (marine) environment. Our results indicate that, due to material properties, spectroscopic methods alone appear to be unsuitable for quantification of coating/paint particles and underestimate their environmental abundance. ICP-MS/MS and an optimized Py-GC/MS approach in combination with multivariate statistics enables a straightforward comparison of the multi-elemental and organic additive fingerprints of paint particles. The approach can improve the identification of unknown particles in environmental samples by an assignment to different typically used coating types. In future, this approach may

* Corresponding author.
E-mail address: daniel.proefrock@hereon.de (D. Pröfrock).

https://doi.org/10.1016/j.jhazmat.2024.134173
Received 31 January 2024; Received in revised form 14 March 2024; Accepted 29 March 2024
Available online 30 March 2024

facilitate allocation of emission sources of different environmental paint/coating particles. Indeed, future work will be required to tackle various remaining analytical challenges, such as optimized particle extraction/separation of environmental coating particles.

1. Introduction

It is estimated that about 40% of all applied paints and coatings are mismanaged and leak into the environment [1]. Hereby, over 60% are emitted in the form of microplastics (MPs; < 5 mm in size). Consequently, paints and coatings are considered a large source of MPs into the ocean and waterways (156–1900 kt/year) with a total estimated emission into the environment between 640 and 9800 kt/year [2,1,3,4]. In a study from Cardozo et al. [5], up to 35% of the synthetic particles found in fish guts were paints [5]. Paint and coating particles are of high ecotoxicological concern, due to their elevated chemical toxicity compared with MPs of similar sizes. High concentrations of hazardous inorganic additives have been used up to now to produce anti-corrosion paints and coatings with specific properties [6]. Harmful ions such as Cu^{2+}, tributyl tin^{+}, Pb^{2+} and CrO_4^{2-} can migrate out of the bulk materials or out of abraded particles on short timescales [6,7]. In contrast to the numerous studies on plastic particles, there is little reliable data on the amount of emissions and the fate of paint and coating particles in the environment [4]. Almost 50% of the paint and coating emissions can be assigned to architectural sources. Other sources include automotive (8%), industrial (24%) and marine (12%) inputs [1]. Although estimates suggest likely emissions of up to 12,000 - 30,000 tons to European surface waters, on-sea emissions of paint/anti-corrosive coating particles have gained little scientific attention [4]. Within this context, the release of chemicals like organic and inorganic additives, as well as particulate pollutants can be accelerated by weathering and the harsh marine environment.

There are various reasons for the lack of systematic studies on the fate of paint and anti-corrosion coating particles in the environment, or the exclusion of such particles in most MP studies. So far paint particles are not included in the guidelines of the Convention for the Protection of the Marine Environment of the North Atlantic (OSPAR Convention) for the monitoring of marine litter. Whereas, current guidelines of the Marine Strategy Framework Directive now explicitly include varnish/paint particles as polymer types for data reporting [8]. Indeed, the analysis of paint particles is particularly challenging. Particles with high mass fractions of inorganic pigments have a higher density than most thermoplastics usually analyzed in MP studies, making the commonly used density separation (e.g., with zinc chloride) more difficult. In addition, the layered structure of the paint chips, to which often rust still adheres, hampers the analysis using spectroscopic or visual methods [4].

Previous studies on the analysis of paint and coating particles mainly used either simple microscopic or advanced (micro)spectroscopic methods, in which individual particles are identified and summed ([4] and publications cited therein). Unfortunately, visual counting methods exhibit a strong human bias, especially regarding small particles, and suffer from a high size detection limit. Spectroscopic analysis of (environmental) MP and paint/coating particles is often impeded by high fluorescence in case of Raman spectroscopy [9-11]. Furthermore, strong and broad absorptions of the included fillers hampers Fourier-transform infrared (FTIR) spectroscopy [9]. While Raman (micro)spectroscopy is suitable to detect inorganic pigments and fillers, FTIR and laser direct infrared (LDIR) imaging are better suited for the detection of binders. Indeed, a mass balance for the calculation of material flows is difficult to carry out with these spectroscopic datasets [12]. Due to the chemical heterogeneity of anti-corrosion coatings, an assessment of the emission levels and the whereabouts of the particles in the environment necessitates complementary chemical-analytical methods in conjunction with material-specific databases [13]. Finally, suitable mass-related analytical methods are required for the calculation of mass balances and differentiation between anti-corrosion coating types. Paints and coatings contain a high share of synthetic polymers (on average 37%) [1]. A combination of pyrolysis–gas chromatography/mass spectrometry (Py-GC/MS) [13-15] and inductively coupled plasma mass spectrometry (ICP-MS) [16-18] can generate mass data for the binders and the metals/metalloids contained in the inherent inorganic additives.

The aim of this work was to create a selective analytical toolbox for the accurate and reliable analysis of anti-corrosion coating particles in environmental samples. This will help to close the current knowledge gaps related to the general role and environmental impact of anti-corrosion coating-based MPs, as well as their contribution to the marine MP pollution. To achieve this, we used a complementary analytical approach based on LDIR, FTIR and Raman spectroscopy, as well as tandem ICP-MS (ICP-MS/MS) and Py-GC/MS combined with statistical data analysis.

2. Materials and methods

2.1. Anti-corrosion coatings

Depending on the material, it was difficult to obtain detailed chemical information from the manufacturer's documentation. Since anti-corrosion coatings are always multi-layer systems, we examined a wide selection of paints used for different technical purposes.

Different virgin materials were analyzed in this study (see SI Table A1). The coatings comprised of 12 2-component (2 C) epoxy resins (EP), one 1 C-EP, three 2 C polyurethane (PUR)/acrylate copolymers (all hexamethylene-diisocyanate (HDI) PUR-based), five 1 C PURs (three methylendiphenyl-isocyanate (MDI) PURs, one HDI-PUR, one unknown), one 2 C MDI-PUR, one 1 C polyacrylate, one 2 C aspartate and one 1 C polysiloxane. Five antifouling paints of unknown polymer types were also analyzed. ICP-MS/MS and Py-GC/MS data for 22 of these coatings are presented in this paper (see SI Table A2, SI Table A3 and SI Table A4). A scratch sample from the coating of a bridge crossing the Elbe-Lübeck canal (Germany; 53.410968, 10.595349) was added to the sample set, called "environmental sample" in the following. Detailed pictures of the bridge, the sample and its layered structure can be found in SI Figure A1. According to the records, the coating of this bridge has been renewed several times historically, the last time in 1983, when a red lead containing epoxy resin primer was applied. As intermediate coating, a micaceous iron oxide containing epoxy resin was used and as top coating a non-specified 2 C-PUR. The entire bridge has since been replaced for technical reasons.

2.2. Py-GC/MS analysis

The Py-GC/MS measurements were performed using a micro-oven pyrolyzer EGA/Py-3030D (FrontierLabs, Japan) with an auto-shot sampler AS-1020E (FrontierLabs, Japan). The pyrolyzer was coupled to an Agilent 7890B gas chromatograph equipped with an Agilent J&W HP-5MS-UI column with an upstream deactivated precolumn. An Agilent 700 C was attached to the gas chromatograph. Detailed information on the measurement parameters can be found in SI Table A5.

Every sample was measured twice, once with direct pyrolysis and once with reactive pyrolysis. For each measurement, 50 μg ± 5 μg of small flakes of the hardened anti-corrosion coatings were separated with a scalpel and weighed into pyrolysis cups (FrontierLabs, Japan) using an ultra-microbalance (XPR2U, Mettler Toledo, USA). Before measuring the samples, 10 μL of poly(4-fluorostyrene) solution (PFS; Polymer Standards Service GmbH, Germany; 200 μg mL^{-1}, as internal standard)

were added to the cups and evaporated at room temperature.

For reactive pyrolysis, 20 µL of tetramethylammonium hydroxide (TMAH; 25% in methanol, Fluka, Germany) were pipetted into the cups and allowed to evaporate at room temperature as well.

Data evaluation was performed with the help of an in-house target-list/database. The database was created with AMDIS (Automated Mass spectral Deconvolution and Identification System; Version 2.73, National Institute of Standards and Technology, NIST, USA). Each entry consists of a mass spectrum, compound name, retention time index (RI) and database ID.

Compounds were tentatively identified using the NIST database (NIST14) and based on literature references [19]. Compounds that could not be identified were labeled 'unidentified' and assigned the respective RI. The database ID was matched to the polymer types for which the compound was detected and to the CAS number of the tentatively identified compound. If no compound could be identified, the database ID was labeled "U" for 'unidentified' complemented by the respective RI. The target library used for data evaluation consisted of eight polymer types (EP, MDI-PUR, PUR-Ac, polyacrylate, polysiloxane, polyaspartate, polystyrene, polycarbonate) and 225 targets.

Pyrograms were evaluated using OpenChrom (Lablicate Edition 1.4.0.202201261344, Germany). For peak detection, a data deconvolution was performed using the MCR-AR (Multivariate Curve Resolution with Alternating Regression) 'targeted chained' function. Targets were identified by comparing the mass spectrum of each identified peak with the mass spectra of the target library using the OpenChrom 'cosine * *m/z*' function. To avoid false positives, targets were only identified if they were in the RI window (RI of the target library entry ± 10). RI calibration was done on every sequence by measuring a PE standard and creating an RI calibration file using OpenChrom. The minimum match factors and reverse minimum match factors for target identification were set to 60, and a manual check/review of each identified target was performed at the end of evaluation. The peak areas of each identified target were calculated using the trapenozoid" function. A peak area ratio was calculated from the peak area of the targets and the peak area of the internal standard (PFS trimer) of each measurement. This ratio was used for statistical analysis.

2.3. ICP-MS/MS analysis

The hardened materials were pre-comminuted with a conventional mortar and pestle, and ground by using a ball mill (Planetary ball mill PM400, Retsch, Germany). Seven agate balls (d = 20 mm) in conjunction with 125 mL agate grinding cups were used. Rotation speed and milling time were set to 400 rpm and 15 – 60 min depending on the materials' brittleness. The coating particles were subjects to microwave-assisted acid digestion (MWAD). Three replicates of 50 mg ± 6 mg (1 *SD*; n = 3) per coating material were weighed into pre-cleaned 55 mL TFM (modified polytetrafluoroethylene (PTFE)) vials (MARS 6, CEM Corp., Germany).

Digestions (40 samples per run) were conducted at 230 °C (ramp time: 20 min; hold time: 60 min; max. power: 950 W) in 4 mL nitric acid (HNO_3; 65% *w/w*, Merck-Millipore), 1 mL hydrochloric acid (HCl) (30% *w/w*, Merck- Millipore) and 1 mL tetrafluoroboric acid (HBF_4) (38% *m/m*, Chem-Lab, Zedelgem, Belgium). P.a. grade HNO_3 and HCl were further purified by double sub-boiling in perfluoroalkoxy alkane (PFA) stills (Savillex, USA). Microwave vessels were cleaned (two times) in a acid steam cleaner at 90 °C for 8 h (65% HNO_3; Easy Trace Cleaner Evolution II, ANALAB, France). After digestion, the solution was quantitatively transferred to a pre-cleaned 50 mL DigiTUBE (SCP Science, Canada) and diluted to a final volume of 50 mL with Milli-Q water. Vacuum-filtration (0.45 µm PTFE filters; SCP Science, Canada) with a manifold was applied to remove any remaining undigested particles. Type I reagent-grade water (18.2 MΩ cm) was obtained from a Milli-Q Integral water purification system (Merck-Millipore, Germany) equipped with a Q-Pod Element and a 100 nm endfilter. Tubes and pipette tips (VWR International, USA) were pre-cleaned in a two-stage washing procedure using diluted HNO_3 (10% *m/m* and 1% *m/m* respectively).

The certified reference materials (CRMs) ERM-EC680m (low density polyethylene (LD-PE); JRC, Ispra, Italy), NMIJ CRM 8133-a (polypropylene (PP); NMIJ, Tsukuba, Japan) and NIST SRM 2582 (powdered paint; nominal Pb mass fraction: 200 mg kg^{-1}) were digested for method validation. A comprehensive overview about mass fractions of certified and non-certified elements for the analyzed reference materials can be found elsewhere [16].

The instrument settings, measured isotopes and chosen measurement modes were very similar to those previously described [16,20]. However, O_2 was replaced by N_2O as reaction gas according to Klein et al. [20]. Multi-elemental analysis covering 55 elements in four different cell modes (no gas, He, N_2O and H_2) was performed using an ICP-MS/MS instrument (Agilent 8800, Agilent Technologies, Japan) coupled to an ESI SC-4 DX FAST autosampler (Elemental Scientific, USA). The instrument was tuned in a daily routine using a Li, Co, Y, Ce, Tl solution. Rh and Ir were used as internal normalization standards (Merck-Millipore, Germany). An in-house quality control multi-elemental standard solution (Inorganic Ventures, USA) was rigorously measured at least five times during each measurement batch.

2.4. Spectroscopic analysis

Coating fragments were scraped off using a ceramic scalpel for further spectroscopic analysis. The same specimen was analyzed using LDIR, Raman and FTIR spectroscopy. Data of the spectroscopic analysis can be found in SI Table A6.

2.4.1. LDIR

The particles were placed on a MirrIR (low-e microscope) slide (Kevley Technologies, USA) and analyzed using the Agilent 8700 LDIR Chemical Imaging system (Agilent Technologies, USA) in transflection mode [21–23]. The instrument's functional principles (quantum cascade laser-based IR imaging in conjunction with an automated spectral database comparison) are described in more detail in previous publications [24,25]. The Agilent Clarity software (version 1.1.2) was used to perform the analysis. The spectral library (Microplastic starter 1.0, Agilent Technologies) was expanded by spectra of environmental particles whose polymer identity was confirmed using the µ-ATR-unit of the system. Additionally, the spectra of in-house reference MPs (expanded polystyrene (EPS), polyethylene (PE), polyethylene terephthalate [26], PP polystyrene (PS) and polyvinylidene chloride (PVDC; similar IR spectrum to polyvinylchloride (PVC)) and different polymeric materials used in the laboratory were integrated into the library (Hereon LDIR Library for Microplastic Analysis) [22,23].

2.4.2. Raman

The particles placed on the MirrIR (low-e microscope) slides (Kevley Technologies, USA) were analyzed by µ-Raman spectroscopy (Senterra, Bruker Optik GmbH, Germany) using a 10 × magnification lens. All spectra (10 accumulations) were measured with an excitation wavelength of 632.8 nm. Laser powers of 5, 10 and 25 mW, and integration times of 5, 10 and 20 s were tested. Raman spectra were evaluated using the R package "RamanMP'' [11]. The Raman spectra were compared to the MP database with 356 spectra (325 of which are additives) which is included in "RamanMP" [27]. Additionally, 208 Raman spectra of pigments (130 spectra of pure pigments, 78 of pigments + acrylic binder) from the pigments checker database (https://chsopensource.org/pigments-checker/) were used for comparison [28].

The fluorescence background was removed from the measured and pigments checker spectra with the R package "baseline" [29] based on modified polynomial fitting [30]. Best results for baseline correction were obtained with a 10th and 16th grade polynomial for measured and pigments checker spectra, respectively. Default settings were used for the other parameters.

The matching of the minimum-maximum normalized sample and reference spectra based on the Pearson correlation coefficient was performed with a matching tolerance of 0.5. For all other parameters, default settings were used. Other tolerance factors (0.25, 0.75) as well as Z-score normalization (instead of minimum-maximum) were also tested but did not significantly change the results of the best matching reference spectrum. The sample spectra were matched separately with the original MP database spectra or the baseline-corrected pigments checker data.

2.4.3. ATR-FTIR

The coating particles were placed on the diamond crystal and analyzed by ATR-FTIR spectroscopy (Alpha I, Bruker Optics, Germany). Measurements were performed three times with 32 scans and a resolution of 4 cm^{-1} (wavenumber range: 4000 cm^{-1} – 400 cm^{-1}). The respective ATR-FTIR spectra were compared to the siMPle single spectra IR (326 spectra) and automated IR analysis (270 spectra) databases (https://simple-plastics.eu) using OPUS (version 7.5, Bruker Optics) [31]. Hereby, the vector-normalized original spectra and their first derivatives were used. To the best of the authors' knowledge, the used IR-database is the most widely used open-source database in microplastics research.

2.5. Multivariate statistics

Statistical evaluations were performed using STATISTICA® (StatSoft, Inc., USA, version 12.5). Variations in the chemical properties of the coating materials were examined by means of a hierarchical cluster analysis, in conjunction with a principal component analysis (PCA). For this purpose, multivariate statistical analyses were performed for both ICP-MS/MS (multi-element dataset: inorganic additives) and Py-GC/MS (characteristic pyrolysis products of polymers: binders) results. Here, the statistical analysis for the Py-GC/MS was conducted twice covering the direct, as well as the reactive pyrolysis.

For all statistical analysis methods, the datasets were subjected to rank transformation to eventually remove possible outliers as well as approximate the data to a normal distribution, additionally all variables with variances equal to zero where neglected.

For the cluster analysis, Ward's method with squared Euclidean distances was chosen. The factor loadings of the PCA were rotated using the varimax procedure. This rotation method allows the loadings of each variable to be restricted to only one factor, thus allowing a better interpretation of the direct relationships between factors and the items based upon them.

3. Results and discussion

3.1. ATR-FTIR, Raman and LDIR data

Table 1 shows results of the spectroscopic analysis of 22 different coating particles via ATR-FTIR, Raman and LDIR analysis. Although the materials were in a virgin state (no photo-oxidation and no biofilm), only small proportions were identified as MPs with a hit quality index (HQI) above an acceptable threshold value (Pearson correlation coefficient $\geq$ 0.65 for the original spectrum or its 1st derivative) [32,33]. SI Table A6 shows the results of the spectroscopic analysis of all coating particles. ATR-FTIR, Raman and LDIR spectroscopy only identified 40%, 10% and 33% of the coating particles as MPs (or MP + pigment), respectively. Due to broad bands in the fingerprint region, likely from fillers such as carbon black and silicon dioxide, ATR-FTIR assigned > 50% of the materials to carbon, while LDIR erroneously identified 2/3 as silica (dominant band at ~ 1280 cm^{-1}). The poor results for Raman spectroscopy and the associated data evaluation routines can be explained by the high share of spectra showing a strong fluorescence background (despite testing of different lasers and energies during optimization). In most cases, this background could not be compensated for by the background correction. However, Raman spectroscopy identified titanium dioxide (TiO_2) in two of the samples (3 and 26; both grey color) and arylide yellow in one sample (20; yellow color) with high HQI values (see SI Table A6). Our results underline that vibration spectroscopy techniques and state-of-the-art databases used in this study are currently unsuitable for the analysis of coating particles. The findings clearly indicate that most MP monitoring studies relying on these techniques significantly underestimate the abundance of paint/coating particles in the environment. Nonetheless, there is evidence that resin (e.g. acrylic or epoxy), adhesive, paint, varnish and polyurethane coating particles are highly abundant in the marine [34,22,23,35] and limnetic environment [36]. The share of such particles seems to increase with decreasing particle size, which increases the potential for ingestion and translocation [22,23]. The application of the determined underestimation (mathematical correction) to existing studies in which paint particles are already one of the most abundant categories would lead to significantly higher particle number concentrations for the respective regions (despite a high uncertainty). Considering the assumed higher toxicity compared to thermoplastic/regular MP particles of similar sizes, the results tend to raise concern. The extension of IR databases could help to reduce the high false negative identification rate. However, many spectra showed very strong absorption or uncharacteristic peaks resulting from mineral fillers. To get a more accurate picture of the occurrence of paint and coating particles in the environment, complementary mass spectrometric techniques were applied in this study.

Table 1
Summary of the spectroscopic analysis of 28 coating particles via ATR-FTIR, Raman and LDIR spectroscopy. * Original spectra and * * 1st derivatives.

Spectroscopic technique	Number /share of MP assignments	Most frequent assignment (number, share) – regardless of threshold value
ATR-FTIR	12/28 (43%)	Carbon (16/28; 57%) * Phenoxy resin (9/28; 32%) * *
Raman	3/28 (11%)	*Pigments checker:* ultramarine natural + acrylic binder (7/28; 25%) * Cadmium red (12/28; 43%) * * *MPdatabase:* PA_2-polyamide (7/28; 25%) * PR209-quinacridone (La Nasa, Doherty et al.) (11/28; 39%) * *
LDIR	10/28 (36%)	Silica (20/28, 71%)

3.2. ICP-MS/MS data

For quality control, the CRMs ERM-EC680m (LDPE), NMIJ CRM 8133-a (PP) and NIST SRM 2582 (powdered white paint), as well as digestion blanks were analyzed for their elemental mass fractions. Recovery rates of certified elemental mass fractions were 87–104% (Cd, Cr, Hg, Pb, Sb, Sn, Zn), 87–113% (Cd, Cr, Hg, Pb) and 93% (Pb). All measured elemental mass fractions of the analyzed reference materials can be found in SI Table A2. Thus, the analytical process including MWAD, filtration and ICP-MS/MS can be regarded suitable for investigating the metal(loid) mass fractions of MP. In total, mass fractions of 55 different metal(loid)s were determined. Table 2 contains mass fractions of selected elements for all analyzed paint particles. SI Table A2 contains mass fractions of all measured elements, expanded uncertainties as well as *LOD*s and *LOQ*s.

The highest mass fractions of As (90,000 μg kg^{-1}), Cr (3,100,000 μg kg^{-1}), Mo (680,000 μg kg^{-1}) and Pb (590,000 μg kg^{-1}) were found in the environmental sample (Env. sample) taken from a bridge crossing the Elbe-Lübeck-Canal. The mass fractions were partly several orders of magnitude above those of the non-environmental samples (maximum Pb: 3800 μg kg^{-1}; maximum Cr: 380,000 μg kg^{-1}; maximum Mo: 5700 μg kg^{-1}; maximum As: 12,300 μg kg^{-1}).

The highest mass fractions of Cd (1500 μg kg^{-1}) were measured in the samples 14 (2 C-PUR) and 11 (2 C-EP). The maximum Zn

Table 2
Measured mass fractions and expanded uncertainties (U(k = 2)) of As, Cd, Co, Cr, Er, La, Mo, Pb, Sr and Zn of all analyzed paint particles. C: component; EP: epoxide; HDI: hexamethylene diisocyanate; MDI: methylene diphenyl diisocyanate; PUR: polyurethane. Values for LODs and LOQs can be found in SI Table A2.

Material information			As	Cd	Co	Cr	Er
#	Colour	Material	w [µg kg^{-1}]	w [µg kg^{-1}]	w [µg kg^{-1}]	w [µg kg^{-1}]	w [µg kg^{-1}]
1	**Blue**	**PUR (HDI)/ acrylate**	170 ± 120	520 ± 190	130 ± 40	*<LOQ*	80 ± 30
2	**Black**	**1 C-PUR (MDI)**	5000 ± 700	*<LOQ*	3900 ± 400	26,000 ± 1800	472 ± 26
3	**Grey**	**2 C-EP**	3200 ± 500	960 ± 140	3480 ± 130	221,000 ± 13,000	1010 ± 140
4	**Light green**	**2 C-PUR**	*<LOD*	*<LOQ*	*<LOQ*	*<LOD*	75 ± 21
5	**Black**	**1 C-PUR**	2100 ± 300	80 ± 50	8800 ± 500	44,800 ± 2000	740 ± 60
6	**yellowish**	**EP (primer)**	*<LOD*	18 ± 22	74 ± 16	*<LOD*	42 ± 6
7	**Grey**	**2 C-EP**	510 ± 290	580 ± 110	490 ± 40	2900 ± 500	153 ± 25
8	**Blue**	**1 C-polyacrylate**	10,500 ± 500	330 ± 110	30,000 ± 2100	16,000 ± 8000	280 ± 50
9	**Grey**	**2 C-EP**	9300 ± 2800	17 ± 25	3500 ± 1900	36,000 ± 9000	310 ± 90
10	**Reddish brown**	**2 C-EP**	1350 ± 230	40 ± 40	1800 ± 150	25,000 ± 1000	1210 ± 150
11	**Grey**	**2 C-EP**	5500 ± 3000	1500 ± 260	5330 ± 220	295,000 ± 21,000	1620 ± 130
13	**Grey**	**1 C-Polysiloxane**	7500 ± 1000	890 ± 130	16,900 ± 700	202,000 ± 13,000	1180 ± 80
14	**White**	**2 C-PUR**	1200 ± 400	1500 ± 150	350 ± 40	*<LOQ*	320 ± 30
15	**Grey**	**1 C-PUR (MDI)**	2900 ± 600	960 ± 170	2300 ± 100	25,100 ± 2500	360 ± 40
17	**Turquoise**	**PUR (HDI)/Acrylate**	12,300 ± 1200	230 ± 80	5100 ± 400	12,400 ± 3000	290 ± 30
19	**Grey**	**2 C-EP**	200 ± 110	810 ± 120	310 ± 40	*<LOQ*	26 ± 8
20	**Yellow**	**2 C -Aspartate**	850 ± 240	380 ± 80	1930 ± 60	69,000 ± 4000	76 ± 10
21	**White**	**2 C-EP**	280 ± 120	360 ± 90	1720 ± 100	*<LOQ*	140 ± 21
22	**Reddish brown**	**2 C-EP**	9100 ± 1200	270 ± 100	10,300 ± 800	380,000 ± 40,000	54 ± 8
23	**Reddish brown**	**2 C-EP**	10,800 ± 600	100 ± 50	22,800 ± 1600	80,000 ± 4000	180 ± 40
24	**White**	**1 C-PUR (HDI)**	230 ± 100	70 ± 40	208 ± 27	*<LOD*	19 ± 5
25	**White**	**2 C-EP**	540 ± 230	500 ± 190	660 ± 90	8600 ± 500	860 ± 110
Env. sample		**-**	90,000 ± 90,000	800 ± 500	16,000 ± 900	3100,000 ± 500,000	35 ± 12
ERM_EC681m		**LD-PE**	17,600 ± 1100	131,000 ± 7000	467 ± 18	41,900 ± 1600	*<LOD*
NMIJ_CRM_8133a		**PP**	*<LOD*	82,000 ± 3000	1080 ± 80	910,000 ± 50,000	*<LOD*
SRM_2582		**paint**	3900 ± 500	3300 ± 400	150,000 ± 21,000	30,000 ± 5000	137 ± 21
Material information			**La**	**Mo**	**Pb**	**Sr**	**Zn**
#	**Colour**	**Material**	***w* [µg kg^{-1}]**	***w* [µg kg^{-1}]**	***w* [µg kg^{-1}]**	***w* [µg kg^{-1}]**	***w* [µg kg^{-1}]**
1	**Blue**	**PUR (HDI)/ acrylate**	1500 ± 500	440 ± 40	*<LOD*	200,000 ± 80,000	10,000 ± 3000
2	**Black**	**1 C-PUR (MDI)**	17,000 ± 1300	2690 ± 260	*<LOQ*	5300 ± 300	11,500 ± 1000
3	**Grey**	**2 C-EP**	18,500 ± 1100	780 ± 100	1660 ± 170	91,000 ± 3000	15,800 ± 2700
4	**Light green**	**2 C-PUR**	223 ± 20	*<LOD*	*<LOQ*	1090 ± 120	2000 ± 400
5	**Black**	**1 C-PUR**	7200 ± 600	5250 ± 180	3400 ± 300	23,800 ± 300	46,900 ± 2900
6	**yellowish**	**EP (primer)**	520 ± 40	30 ± 17	*<LOQ*	2630 ± 140	2900 ± 400
7	**Grey**	**2 C-EP**	3700 ± 500	340 ± 60	1190 ± 110	500,000 ± 40,000	34,500 ± 2700
8	**Blue**	**1 C-polyacrylate**	2100 ± 150	3830 ± 260	1900 ± 400	1373,000 ± 25,000	200,000 ± 40,000
9	**Grey**	**2 C-EP**	5800 ± 2600	5700 ± 2600	*<LOQ*	9000 ± 4000	6200 ± 2300
10	**Reddish brown**	**2 C-EP**	12,700 ± 1000	4400 ± 400	1590 ± 220	11,100 ± 500	12,200 ± 800
11	**Grey**	**2 C-EP**	22,800 ± 1300	2100 ± 1400	1160 ± 110	153,000 ± 4000	22,000 ± 5000
13	**Grey**	**1 C-Polysiloxane**	16,200 ± 700	1680 ± 140	3800 ± 400	121,000 ± 4000	8900 ± 800
14	**White**	**2 C-PUR**	3280 ± 180	680 ± 70	3410 ± 290	6300 ± 400	139,000 ± 7000
15	**Grey**	**1 C-PUR (MDI)**	14,800 ± 400	2100 ± 400	1540 ± 100	397,000 ± 15,000	22,700 ± 1100
17	**Turquoise**	**PUR (HDI)/Acrylate**	4100 ± 700	4900 ± 400	820 ± 110	85,000 ± 7000	9400 ± 800
19	**Grey**	**2 C-EP**	295 ± 27	360 ± 70	*<LOD*	59,900 ± 1700	3670 ± 200
20	**Yellow**	**2 C -Aspartate**	910 ± 70	230 ± 60	*<LOQ*	147,000 ± 5000	19,300 ± 1300
21	**White**	**2 C-EP**	1070 ± 120	420 ± 100	1160 ± 120	2690 ± 150	239,000 ± 14,000
22	**Reddish brown**	**2 C-EP**	360 ± 60	390 ± 40	*<LOQ*	14,500 ± 1300	13,500 ± 900
23	**Reddish brown**	**2 C-EP**	2720 ± 290	15,500 ± 500	7400 ± 500	4560,000 ± 220,000	27,900,000 ± 1500,000
24	**White**	**1 C-PUR (HDI)**	85 ± 16	32 ± 17	*<LOD*	30,900 ± 1400	*<LOQ*
25	**White**	**2 C-EP**	8100 ± 700	350 ± 90	1490 ± 180	1090,000 ± 70,000	53,000 ± 4000
Env. sample		**-**	1070 ± 190	680,000 ± 110,000	59,000,000 ± 6000,000	1150,000 ± 90,000	128,000 ± 10,000
ERM_EC681m		**LD-PE**	*<LOD*	22 ± 25	72,000 ± 6000	*<LOD*	1020,000 ± 30,000
NMIJ_CRM_8133a		**PP**	*<LOD*	*<LOD*	1080,000 ± 110,000	*<LOD*	93,000 ± 4000
SRM_2582		**paint**	2700 ± 500	1230 ± 130	190,000 ± 40,000	740,000 ± 130,000	4700,000 ± 400,000

(27,900,000 µg kg^{-1}) and Sr mass fraction (4,560,000 µg kg^{-1}) were determined for sample 23 (2 C-EP). In sample 8 (1 C-polyacrylate), the highest Co (30,000 µg kg^{-1}) mass fractions were measured. La was measured over a range from 85 to 22,800 µg kg^{-1}, while Er mass fractions spanned from 19 to 1620 µg kg^{-1}. For both elements, the maximum was found in sample 11 (2 C-EP).

Multivariate statistical analyses on the multidimensional ICP-MS/MS dataset highlighted correlations and revealed invisible information about the samples and their interrelationships. Detailed data on the statistical analysis of the ICP-MS/MS for alle analyzed 55 metal(loid)s can be found in SI Table A7. PCA yielded five factors (F1 – F5) describing 79.3% of the explanatory variance of the studied samples. Each of these five factors exhibited elevated to high loadings on certain characteristic elements: F1: Heavy rare earth elements (HREEs), Y, Th, light rare earth elements (LREEs), Be; F2: Co, As, Fe, Ni, Mn; F3: Zr, Cd, Ag, Ti, Ge; F4: Ba, Sr, Cu, Mg, Sc; F5: Na, Sn, Sc, Ca, V.

As shown in Fig. 1, F1 separates cluster 3 (green star) from cluster 1 (blue triangle) and cluster 2 (yellow circle), while F2 separates cluster 1 (blue triangle) and cluster 3 (green star) from cluster 2 (yellow circle). F3 yields no clear distinction. F4 enables a separation between cluster 1 (blue triangle) and 3 (green star). F5 slightly differentiates cluster 4 (red square) from the other ones.

The samples split up into four stable clusters as shown in Fig. 2. The most important finding is that cluster analysis of the multi-elemental data does not enable a clear differentiation according to color, polymer type, or coating type. All four clusters contain EP- and PUR-based coating materials. Compared to other MPs, e.g. secondary MPs stemming from plastic products with short product lifespans, coatings exhibit

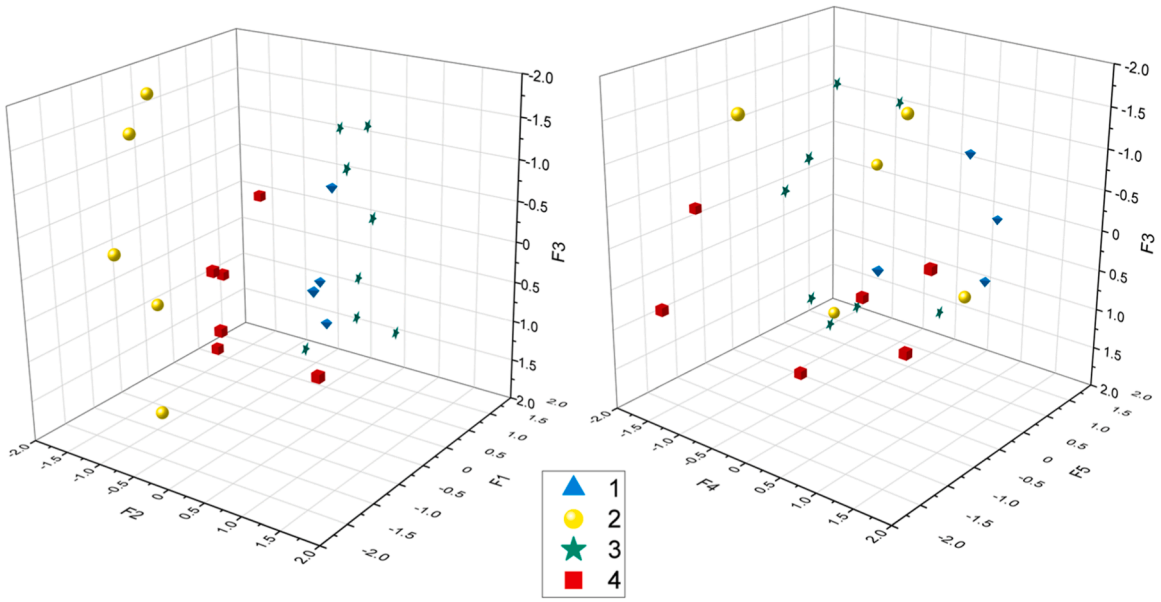

Fig. 1. Representation of the samples' factor loadings in three-dimensional space for the anti-corrosion coating materials based on the multi-elemental dataset generated using ICP-MS/MS. Blue triangle: Cluster 1; Yellow circle: Cluster 2; Green star: Cluster 3; Red square: Cluster 4. (For interpretation of the references to color in this figure legend, the reader is referred to the web version of this article.)

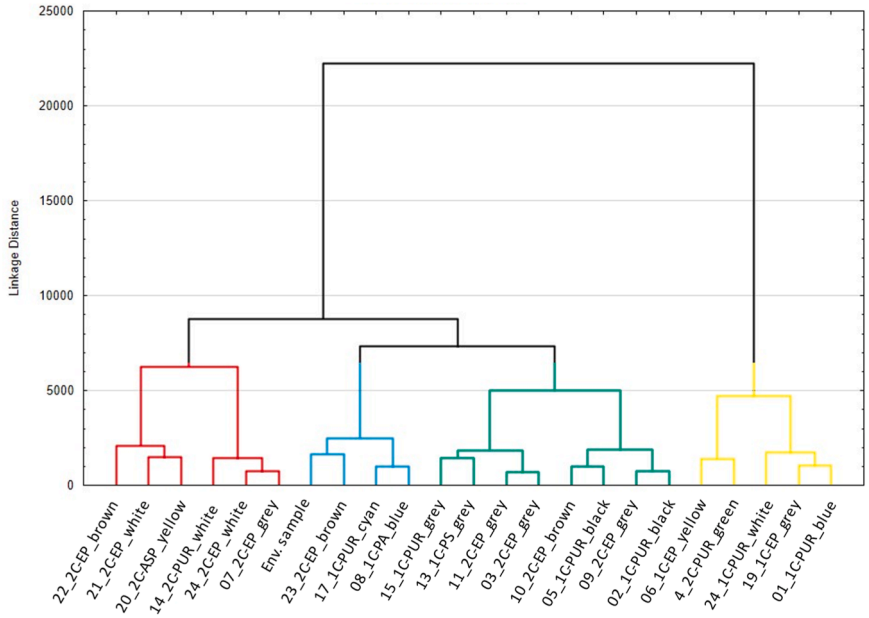

Fig. 2. Results of the cluster analysis (Ward's method, squared Euclidian distances) for the anti-corrosion coating materials based on the multi-elemental dataset generated using ICP-MS/MS. Blue: Cluster 1; Yellow: Cluster 2; Green: Cluster 3; Red: Cluster 4. Labeling includes sample #, material (C: component; ASP: aspartate; EP: epoxide; PS: polysiloxane; PUR: polyurethane) and color. (For interpretation of the references to color in this figure legend, the reader is referred to the web version of this article.)

a low polymer content (on average 37%) [1]. This leads to the addition of a high number of different pigments and functional additives (e.g., to enhance anti-corrosion and/or antifouling properties) to the different binder types (no specific correlation). This leads to partially high mass fractions of the different analyzed elements in the coating materials.

The analyzed environmental sample comprised of five layers with the two main layers probably consisting of an old red paint dating back to 1983. This color contains Pb_3O_4 (II, IV) which was a widely used anti-corrosion pigment (red lead). This could also explain the red-brown color of the sample [26]. In addition to the main layers, the sample also consists of a grey EP-based protective layer, which could explain the high mass fraction of Cr. Catrouillet *et al.* reported that Cr and Pb were used in investigated plastic particles as different pigment compounds to achieve a grey to black color [37]. Additionally, chromate-based compounds (mainly Cr (VI)) have excellent anti-corrosion properties. Therefore, such compounds have been used as additives for a variety of corrosion protection applications. It is noteworthy that hexavalent chromium can also be toxic and carcinogenic, why it has been substituted in many cases [38]. Due to the reduction of chromates in corrosion protection for environmental reasons, alternatives containing various rare earths elements (REEs) were developed [38]. REE-based anti-corrosion additives like $CeCl_3$ or $La(NO_3)_3$ seem to be a promising

alternative to chromate to achieve corrosion protection [38]. Another alternative is sodium molybdate (Na_2MoO_4), as a less toxic and more environmentally friendly corrosion inhibitor [39]. Experiments with $BiVO_4$ as corrosion inhibitor are described in the literature [40]. Moreover, $BiVO_4$ is used as a yellow pigment [37]. However, the mass fractions of Bi and V in the coating materials revealed a minimal molar ratio of 2.84, which is not in accordance with the pigment $BiVO_4$. Lead chromate ($PbCrO_4$) is also used as a yellow pigment and exhibits positive material properties [41]. Based on the determined mass fractions, a minimal molar ratio of 3.69 was calculated, which does not match $PbCrO_4$. In both cases the measured elemental ratios do not rule out the presence of $BiVO_4$ or $PbCrO_4$, but rather proof the presence of other sources of Bi, V, Pb and/or Cr in the coating, thus leading to elemental ratios different than the pigments $BiVO_4$ and $PbCrO_4$.

Other uses of metal salts as additives include Mn(IV) oxide as a grey pigment [37]. Mn is also used in combination with Cd as a pigment, but fortunately no high mass fractions of Cd were determined in the analyzed paint samples. In the literature, the use of As-compounds as biocides in antifouling coatings and paints is described. Even if these compounds no longer meet today's environmental standards, there could be a possible connection with the mass fractions in the environmental sample [42].

The samples 7 and 14, which showed a grey to white color, contained very high Ti mass fractions (19,500,000 ± 1,900,000 μg kg^{-1} (2% *w/w*) and 50,000,000 ± 4,000,000 μg kg^{-1} (5% *w/w*) (U ($k = 2$); $n = 3$)). Interestingly, Raman spectroscopy did not reliably (low HQI values) detect TiO_2 in these materials. In sample 3, which also exhibited a high Ti mass fraction (13,900,000 ± 1,500,000 μg kg^{-1} (1.42% *w/w*)), TiO_2 / Titanium white was detected with high confidence (SI Table A5). SRM 2582, which is powder of a historic white color (with comparably high Pb mass fractions), contains a Ti mass fraction of 15% *w/w*. TiO_2 is used as a pigment, also known as titanium white. It is applied in coating materials [43] and sunscreens [44] since it features „UV–absorbing-stabilizing properties" [41,43]. TiO_2-nanoparticles (NPs) have been considered inert for a long time until different in vitro studies have shown that TiO_2-NPs are cyto- and genotoxic. Consequently, the International Agency for Research on Cancer (IARC) has classified TiO_2-NPs as possibly carcinogenic to humans [45,46].

The analyzed materials contained low mass fractions of regulated heavy metals. Future studies should investigate whether the coatings can release other ecotoxicologically relevant elements such as Cr, Cu or Zn but also TiO_2-NPs in relevant quantities. As the example of Cr shows, the determination of the respective species is of importance in this context.

3.3. Py-GC/MS data

Data analysis of direct and reactive Py-GC/MS pyrograms was performed using the 225 targets included in the BSH in-house database. Of the 225 targets, between 15 and 54 targets per measurement were identified for direct pyrolysis and between 16 and 76 targets per measurement for reactive pyrolysis (SI Table A11).

Via direct pyrolysis, epoxy resins have been identified by small aromatic pyrolyzates (e.g. benzene, toluene, *o*-cresol, *p*-cresol, indene) combined with phenolic compounds such as *p*-isopropenylphenol, *p*-isopropylphenol, 4-(1-methyl-1-phenylethyl)phenol or *p*-hydroxy-3-methyl-2,2-diphenylpropane. During reactive pyrolysis, the presence of TMAH leads to the formation of several methyl ethers, with anisole, *o*-isopropylanisole, 1-methoxy-4-(2-phenylpropan-2-yl)benzene and especially bisphenol A dimethyl ether always being detected. The compounds 1-methoxy-2-((4-methoxyphenyl)methyl)benzene, 2-(4′-methoxyphenyl)− 2-(2′-methoxy-phenyl)propane, 2-(4′-methoxyphenyl)− 2-(3′-methyl-4′-methoxyphenyl)propane, 4,4′-dimethoxydiphenyl methane and bis(3-methoxyphenyl)methane were frequently detected as well and helped in the identification of epoxy resins.

Polycarbonates (PC) are structurally quite similar to epoxy resins, e. g. they both share bisphenol A as main component and show a similar thermal degradation behavior. Therefore, pyrolysis markers are also similar for PC and epoxy resins. Polycarbonate products were additionally measured by direct and reactive pyrolysis. The results show that only the unidentified RI1452 and *o*-isopropylanisole were detected in two different PC samples (SI Table A11), so that the unidentified compounds (RI2323, RI2357 and RI2249) can be used to distinguish between EP coating and PC microplastic particles.

Based on the in-house database, the polyaspartate sample (sample 20) was classified as epoxy resin by both direct and reactive pyrolysis. All typical epoxide markers were identified. No significant additional, unidentified peaks were observed in the pyrograms that could refine the result. To our current knowledge, polyaspartates were not yet analyzed by Py-GC/MS in other studies. For a more reliable identification, a larger number of various polyaspartate coating products need to be analyzed to identify characteristic markers to distinguish the polymer from epoxy resins.

The MDI-PUR coating products were identified primarily by the presence of 3,3′-methylenedianiline and 4,4′-methylenedianiline, the pyrolyzates of the monomer methylenediphenyl diisocyanate, in the direct pyrolysis. These pyrolyzates are partially derivatized in reactive pyrolysis, so that 4,4′-methylenebis(2-methylaniline), 4,4′-methylenebis (*N*-methylaniline), *N*,*N*-dimethyl-4-((4-(methylamino)phenyl)methyl) benzenamine and 4,4′-methylenebis(*N*,*N*-dimethylaniline) were also detected. These compounds are quite characteristic pyrolysis markers for MDI-PUR which, to our knowledge, do not overlap with any similar polymer.

The identification of polyurethane/acrylate copolymers (PUR-Ac) coatings was based on the simultaneous presence of methacrylates (methyl methacrylate, butyl methacrylate), pyrolyzates known from polystyrene-containing polymers (e.g. styrene, polystyrene dimer and trimer) and several targets listed in the in-house database as unidentified compounds (e.g. unidentified RI2024, unidentified RI2445, unidentified RI2453) in both, direct and reactive pyrolysis.

Pyrolyzates directly attributable to the HDI-PUR content in these samples were not identified as they are not present in the in-house database. It is likely that some of the unidentified compounds listed above represent this fraction. The environmental sample taken from a coated bridge was identified as PUR-Ac coating. However, in contrast to the two pristine PUR-Ac coating samples, the pyrograms of the bridge sample also showed a number of epoxy markers. This may result from an epoxy coating which was used as primary layer and which might partly adhere to the PUR-Ac top coating.

Similar to PUR-Ac, polyacrylate shows methacrylate and styrene based markers. However, unlike PUR-Ac, the polyacrylate sample showed higher relative levels of methacrylate and especially butyl methacrylate and did not contain the "unidentified compounds" detected in PUR-Ac. These differences in characteristic pyrolysis markers can help to distinguish PUR-Ac from polyacrylate.

Direct and reactive pyrolysis identified a mixture of epoxy and primarily PUR-Ac target for sample 13. In the technical data sheet this coating is described as a 1 C high solid topcoat and the safety data sheet discloses significant amounts of triethoxyvinylsilane in its formulation. However, no silicone-containing targets were identified, resulting in a misclassification of sample 13.

Multivariate statistical analysis was performed on both datasets resulting from the direct and reactive pyrolysis. Data on the statistical analysis of the reactive pyrolysis dataset can be found in SI Table A8. Whereas data of the direct pyrolysis can be found in SI Table A9. Indeed, the selectivity of the statistical analysis was higher for the reactive compared to the direct pyrolysis. Therefore, results of the reactive pyrolysis are discussed in detail.

The cluster analysis of the reactive pyrolysis dataset revealed three clusters that can be clearly linked to the polymer type of the coatings. Cluster 1 contains MDI-PUR and polyacrylate samples while cluster 2 includes all PUR-Ac copolymer and the silicone coating samples, which

showed predominantly PUR-Ac targets, as well as the environmental sample from the bridge. Cluster 3 includes the epoxy coatings, and the polyaspartate sample (see Fig. 3).

The PCA yielded ten factors (F1 - F10) describing 80.5% of the explanatory variance of the samples analyzed by reactive Py-GC/MS. Each of these ten factors showed high to very high loadings on certain compounds. Detailed data on the PCA analysis of the reactive Py-GC/MS data set are presented in SI Table A8.

The PCA showed, that the three different clusters described above can already be well differentiated by three factors (F1, F2 and F3), as shown in Fig. 4. For a more detailed differentiation, also within the clusters, additional factors need to be considered, though.

Cluster 3, and therefore all epoxy samples, are largely loaded by factors F1, F3, F6 and F9. Factor F1 is essential to distinguish cluster 3 from the other two clusters and consists entirely of unidentified epoxy compounds, with the exception of *o*-isopropylanisole. These compounds were detected for each product within this cluster and also exclusively for this cluster of coatings. Therefore, these compounds can be very helpful to identify particles from epoxy coatings in environmental samples.

In contrast, the compounds representing factor F3 were detected almost exclusively for sample 9 during reactive pyrolysis leading to the separation of this sample from all other samples within cluster 3 (see Fig. 4). According to the safety data sheet, sample 9 contains significant amounts of cashew nutshell liquid which is mainly characterized by alkyl phenol molecules with a saturated/unsaturated C15 chain at position 3 [47]. Therefore, this ingredient in the 2 C-EP coating is probably represented by the measured component (Z)− 3-(pentadec-8-en-1-yl) phenol, one of the components of factor F3. Factor F6 further separates the samples 3, 10, 11, 20 and 22 within cluster 3. As this factor mainly includes unidentified epoxide targets, it is difficult to discuss the differences between the samples in detail.

The factors F2 and F5 mainly influence cluster 2. In contrast to cluster 1, factor F2 loads negatively on cluster 2, which allows a selective differentiation between the two clusters. Factor F2 includes one of the previously described unidentified compounds typical of PUR-Ac (*unidentified RI2024*) as well as *unidentified RI1938* and benzene compounds with alkyl or alkenyl groups (1,2,4-trimethylbenzene, 1-methyl-4-propylbenzene, 2-propenylbenzene). All compounds from factor F2 were observed for the two pristine PUR-Ac coating products (sample 1 and 7) which shows that PUR-Ac components may be well-defined in environmental samples by these compounds in reactive pyrolysis. Indeed, some of the latter compounds can also be observed for the polymer polystyrene. Since polystyrene MPs can be present in environmental samples at relevant levels, interferences could occur regarding these compounds. Therefore, additional compounds need to be considered to separate PUR-Ac and polystyrene particles when analyzing environmental samples with reactive pyrolysis. For this purpose, the combination of unidentified compounds and styrene- and methacrylate-derived compounds (methyl methacrylate, butyl

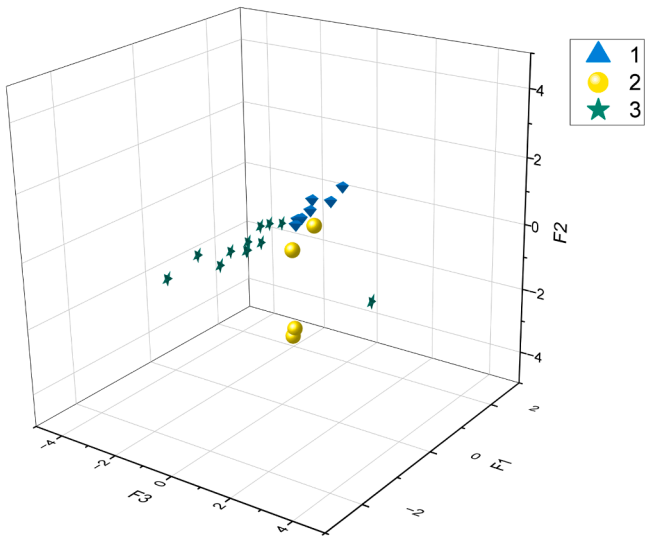

Fig. 4. Representation of the samples' factor loadings in three-dimensional space for the anti-corrosion coating materials based on the Py-GC/MS dataset (11 selected pyrolysis products). Blue triangle: Cluster 1; Yellow circle: Cluster 2; Green star: Cluster 3. (For interpretation of the references to color in this figure legend, the reader is referred to the web version of this article.)

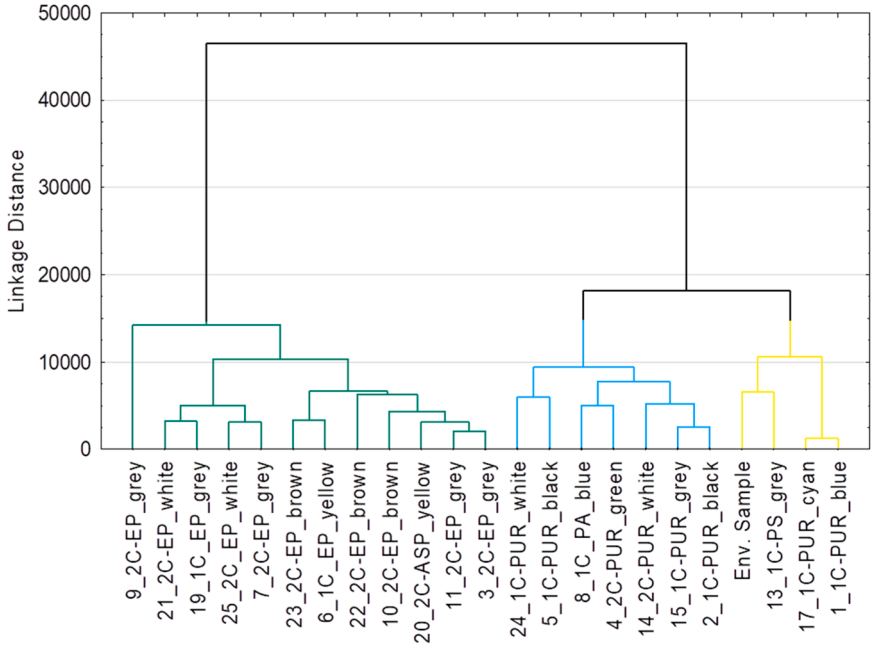

Fig. 3. Results of the cluster analysis for the anti-corrosion coating materials based on the Py-GC/MS dataset (11 selected pyrolysis products). Blue: Cluster 1; yellow: Cluster 2, green: Cluster 3. Labeling includes sample #, material (C:component; ASP: aspartate; EP: epoxide; PS: polysiloxane; PUR: polyurethane) and color. (For interpretation of the references to color in this figure legend, the reader is referred to the web version of this article.)

methacrylate) seems to be more suitable for the identification of PUR-Ac.

For the environmental sample, only the PUR-Ac typical compound *unidentified RI2024* was detected from the compounds of F2. This might be related to a different formulation of the product. As mentioned above, epoxy markers were also identified for the environmental sample as part of the lower epoxy coating layers that might adhere to the top coating. However, these specific epoxy markers were not decisive for any of the factors detected in the multivariate statistical analysis. This is why the environmental sample was unambiguously classified into the PUR-Ac cluster and has no overlap with the epoxy cluster. Still, different coating layers may be identified in environmental samples using reactive pyrolysis.

In contrast to the other PUR-Ac samples, the pyrograms of the silicon coating sample, misclassified into cluster 1 as described above, did not show any of the PUR-Ac typical compounds. Therefore, these could be good indicators to distinguish between the two groups within cluster 1 (PUR-Ac and silicones). However, for the silicone sample a large number of PUR-Ac, but also epoxy targets were classified making it difficult to clearly distinguish this polymer. The used database for silicone corrosion protection products is probably too small (only one product) for reliable identification and differentiation requires a broader dataset.

Factor F5 has a positive and negative load on the PUR-Ac/silicon coating cluster. All compounds are exclusively detected for the environmental sample and comprise unidentified compounds (RI1146, RI1185, RI1282) as well as two chloromethylbenzamines (3-chloro-2-methylbenzenamine and 3-chloro-4-methylbenzenamine). Chloromethylbenzenamines are known pyrolysates of azo dyes [14], which links to the red color of the sampled bridge. For example, 3-chloro-2-methylbenzenamine has already been detected as a pyrolysis product of a red dye with azo pigments [48].

Cluster 1 is significantly influenced by factors F1 (positive), F2 (positive), F4, F7, F8 and F10. None of the MDI-PUR markers used for the identification of samples, such as the MDI derivatives, are relevant for these factors. Compounds of factor F4, including two phthalates which are common plasticizers [49], were exclusively detected for sample 24. In contrast to the other analyzed anti-corrosion coatings, sample 24 is a pasty, polyurethane adhesive intended for applications for high dynamic, structural bonding in marine and boat building according to the technical data sheet. This may be reflected in a different choice with respect to plasticizers in this coating.

Factors F7 and F8 consist of compounds found almost exclusively in sample 4 and 14, respectively. It is difficult to interpret the formation of these factors as no distinct differences for these coatings are known, nor do the pyrolyzates give any indication. The only pyrolyzates that could be traced back to their function are *p*-toluenesulfonamide (sample 4) and its derivative (sample 14), which are used as plasticizers and/or fungicides in paints and coatings [50]. Also, *N*,*N*,*N*′,*N*′-tetramethylbenzidine (sample 4), the reactive pyrolysis product of benzidine, is known to be a compound used to make a variety of azo dyes which may link to the light green color of this coating.

Factor F10 comprises compounds such as butyl methacrylate, 2,2,4-trimethyl-1,3-pentanediol diisobutyrate, bibenzyl, 3-methyleneheptane and 2-ethylhexanal which were all identified for the polyacrylate sample (8) in this cluster only. Of these compounds, butyl methacrylate and bibenzyl were also detected for the PUR-Ac samples in cluster 1 which shows the similarity of sample 8 to PUR-Ac due to the acrylate share of the co-polymer.

3.4. Required future work

This paper only deals with the last two stages of the analytical chain, the chemical analysis and data evaluation of paint/coating particles. For the analysis of environmental samples, for example from the marine environment, efficient and selective extraction/separation methods must be applied upstream to ensure a reliable quantification of particles. Particles > 300 µm or > 500 µm, as considered in this paper, can be isolated from environmental samples e.g. using special forceps and a stereomicroscope, while smaller particles would have to be subjected to chemical or enzymatic digestion (or a combination) with subsequent density separation to be separated from the sample matrix. Furthermore, a significant enrichment would be mandatory for the analysis of smaller particles by ICP-MS and Py GC/MS, especially for aquatic samples.

The extent of matrix-based interferences of e.g. natural organic particles, biofilm formation and non-coating MPs on the analytical results of the described (micro)spectroscopic and mass spectrometry methods must be carefully evaluated. However, this would exceed the scope of this manuscript. Corresponding validation experiments focusing on the sample preparation and its influence on the quantification by (micro)spectroscopic and mass spectrometry methods are and will be conducted in the framework of future work.

Additionally, the extension of the toolbox to include electron microscopy, apart from microscopy based on vibrational spectroscopy, would be beneficial, e.g. to elucidate very small structures and impurities. Laser ablation ICP-MS or µ-XRF could also be helpful to study the distribution of inorganic additives as well as impurities.

4. Conclusion

The overall use of protective anti-corrosion coatings will increase in the coming decades due to increased global ship traffic and the large-scale installation of offshore wind farms in the frame of the ongoing energy transition towards renewable energy in the EU and many other countries. Many of these coatings need to be repaired regularly since they are released into the environment in particulate form because of corrosion, and UV- and mechanical weathering. We present a suitable toolbox to study the release and fate of such particles in the (marine) environment. Especially the optimized Py-GC/MS method in conjunction with multivariate statistical analysis proofed its high potential for identification of coating particles, presupposing that the investigated polymer types and additives are part of the in-house database, which is still being expanded. Typical pyrolyzates characterizing the different coatings can be identified using reactive pyrolysis which are very useful to differentiate the coatings in environmental samples. Furthermore, even specific ingredients, like plasticizers may be identified via specific compounds and may reveal even more information on the composition of environmental samples. Additionally, multi-elemental analysis confirmed that the analyzed anti-corrosion coating materials contain significant mass fractions of ecotoxicologically relevant metal(oid)s which will be released into the environment.

Within the context of source tracing, multivariate statistics might enable a straightforward comparison of the multi-elemental fingerprints of paint particles sampled in the marine environment with the organic additive fingerprints of the coating materials analyzed in this study. A statistical evaluation of the combined organic and inorganic data sets showed no added value compared to the optimized method based only on Py-GC/MS data. The developed approach will also help to improve the identification of unknown particles in environmental or at least its first assignment to the different typically used coating types. In future, this approach may facilitate allocation of emissions sources (e.g. shipping vs. offshore, vs. others) of different environmental coating particles. Significant future work will be required to tackle various remaining analytical challenges. The presented approach does work for large particles and fragments that can be easily isolated from the environment. However, for particles < 300 µm, a suitable extraction process from the respective sample matrix is required. The development of this protocol (selective, contamination-minimized, and mild towards coating and contained additives) would complete the presented toolbox. Additionally, the relevant (micro)spectroscopic methods and corresponding databases should be refined to reduce the underestimation rate of such particles in environmental samples as much as possible.

Environmental implication

Potentially hazardous particles from paints and functional coatings are an overlooked fraction of microplastics (MPs) pollution. Paint and coating particles are of high ecotoxicological concern due to the elevated chemical toxicity compared with MPs of similar sizes. High concentrations of hazardous additives have been historically and are currently used to produce paint and coatings. Our findings indicate that most MP monitoring studies relying solely on spectroscopic techniques significantly underestimate the abundance of paint/coating particles in the environment. Considering the assumed higher toxicity compared to thermoplastic/regular MP particles of similar sizes, the results tend to raise concern.

CRediT authorship contribution statement

Torben Kirchgeorg: Project administration, Funding acquisition. **Elena Hengstmann:** Writing – review & editing. **Alexa Zonderman:** Writing – review & editing. **Anna Siems:** Investigation, Formal analysis. **Ferris Fensky:** Investigation. **Tristan Zimmermann:** Writing – original draft, Supervision, Conceptualization. **Ole Klein:** Writing – review & editing, Visualization, Supervision, Formal analysis. **Marten Fischer:** Writing – original draft, Validation, Investigation. **Lars Hildebrandt:** Writing – original draft, Validation, Supervision, Investigation, Conceptualization. **Daniel Pröfrock:** Writing – review & editing, Project administration, Funding acquisition, Conceptualization.

Funding

Lars Hildebrandt and Ole Klein acknowledge funding of the project P-LEACH from the Helmholtz Association, Innovation Pool of the Research Field Earth and Environment in support of the Research Program “Changing Earth – Sustaining our Future”.

Alexa Zonderman and Elena Hengstmann were funded by the project ANEMOI, an Interreg North Sea project co-funded by the European Union.

Anna Siems was funded through the project CARBOSTORE (grant number: 03F0875A) by the German Federal Ministry of Education and Research (BMBF).

Marten Fischer was funded by the German Federal Ministry of Digital and Transport (BMDV) in the context of the BMDV Network of Experts.

Declaration of Competing Interest

The authors declare that they have no known competing financial interests or personal relationships that could have appeared to influence the work reported in this paper.

Data availability

Data will be made available on request.

Acknowledgements

The authors are grateful to Dr. Thomas Emmler and Silvio Neumann from the Institute of Polymer Research at the Helmholtz-Zentrum hereon for the access to ATR-FTIR and Raman spectroscopy.

Appendix A. Supporting information

Supplementary data associated with this article can be found in the online version at doi:10.1016/j.jhazmat.2024.134173.

References

[1] Paruta, et al., 2022. Plastic paints the environment. EA Environ Action.
[2] Boucher, J. , D. Friot2017. Primary microplastics in the oceans: a global evaluation of sources.
[3] Ryberg, M., A. Laurent , M.Z. Hauschild2018. Mapping of global plastic value chain and plastic losses to the environment: with a particular focus on marine environment. United Nations Environment Programme.
[4] Turner, A., 2021. Paint particles in the marine environment: an overlooked component of microplastics. Water Res X 12, 100110.
[5] Cardozo, A.L.P., Farias, E.G.G., Rodrigues-Filho, J.L., Moteiro, I.B., Scandolo, T.M., Dantas, D.V., 2018. Feeding ecology and ingestion of plastic fragments by Priacanthus arenatus: what’s the fisheries contribution to the problem? Mar Pollut Bull 130, 19–27.
[6] Rees, A.B., Turner, A., Comber, S., 2014. Metal contamination of sediment by paint peeling from abandoned boats, with particular reference to lead. Sci Total Environ 494-495, 313–319.
[7] Eklund, B., Johansson, L., Ytreberg, E., 2014. Contamination of a boatyard for maintenance of pleasure boats. J Soils Sediment 14 (5), 955–967.
[8] Galgani, F., Ruiz-Orejón, L.F., Ronchi, F. et al. 2023. Guidance on the monitoring of marine litter in European seas. An update to improve the harmonised monitoring of marine litter under the Marine Strategy Framework Directive, EUR 31539 EN, Publications Office of the European Union, Luxembourg, 2023, JRC133594, ISBN 978–92- 68–04093-5. Available from: doi:10.2760/59137.
[9] Bouchard, M., Rachel, R., Carrie, M., Learner, T., 2009. Micro-FTIR and micro-Raman study of paints used by Sam Francis. E-Preserv Sci **6**.
[10] Lenz, R., Enders, K., Fischer, F., Brandt, J., Fischer, D., Labrenz, M., 2021. Measuring impacts of microplastic treatments via image recognition on immobilised particles below 100 µm. Microplast Nanoplast 1 (1), 12.
[11] Nava, V., Frezzotti, M.L., Leoni, B., 2021. Raman spectroscopy for the analysis of microplastics in aquatic systems. Appl Spectrosc 75 (11), 1341–1357.
[12] Primpke, S., Fischer, M., Lorenz, C., Gerdts, G., Scholz-Böttcher, B.M., 2020. Comparison of pyrolysis gas chromatography/mass spectrometry and hyperspectral FTIR imaging spectroscopy for the analysis of microplastics. Anal Bioanal Chem 412 (30), 8283–8298.
[13] Bonaduce, I. , A. Andreotti2009. Py-GC/MS of organic paint binders. Organic mass spectrometry in art and archaeology. p. 303–26.
[14] Ghelardi, E., Degano, I., Colombini, M.P., Mazurek, J., Schilling, M., Learner, T., 2015. Py-GC/MS applied to the analysis of synthetic organic pigments: characterization and identification in paint samples. Anal Bioanal Chem 407 (5), 1415–1431.
[15] La Nasa, J., Doherty, B., Rosi, F., Braccini, C., Broers, F.T.H., Degano, I., et al., 2021. An integrated analytical study of crayons from the original art materials collection of the MUNCH museum in Oslo. Sci Rep 11 (1), 7152.
[16] Hildebrandt, L., von der Au, M., Zimmermann, T., Reese, A., Ludwig, J., Pröfrock, D., 2020. A metrologically traceable protocol for the quantification of trace metals in different types of microplastic. PLoS One 15 (7), e0236120.
[17] Hobbs, A.L., Almirall, J.R., 2003. Trace elemental analysis of automotive paints by laser ablation–inductively coupled plasma–mass spectrometry (LA–ICP–MS). Anal Bioanal Chem 376 (8), 1265–1271.
[18] Le Bot, B., Arcelin, C., Briand, E., Glorennec, P., 2011. Sequential digestion for measuring leachable and total lead in the same sample of dust or paint chips by ICP-MS. J Environ Sci Health, Part A 46 (1), 63–69.
[19] Shin, T., Hajime, O., Chuichi, W., 2011. Part 2 - pyrograms and thermograms of 163 high polymers, and MS data of the major pyrolyzates. In: Shin, T., Hajime, O., Chuichi, W. (Eds.), Pyrolysis–GC/MS data book of synthetic polymers. Elsevier, Amsterdam, pp. 7–335.
[20] Klein, O., Zimmermann, T., Pröfrock, D., 2021. Improved determination of technologically critical elements in sediment digests by ICP-MS/MS using N2O as a reaction gas. J Anal Spectrom 36 (7), 1524–1532.
[21] Hansen, J., Hildebrandt, L., Zimmermann, T., El Gareb, F., Fischer, E.K., Pröfrock, D., 2023. Quantification and characterization of microplastics in surface water samples from the Northeast Atlantic Ocean using laser direct infrared imaging. Mar Pollut Bull 190, 114880.
[22] Hildebrandt, L., F. El Gareb , D. Pröfrock 2022. Hereon LDIR library for microplastic analysis.
[23] Hildebrandt, L., El Gareb, F., Zimmermann, T., Klein, O., Kerstan, A., Emeis, K.-C., et al., 2022. Spatial distribution of microplastics in the tropical Indian Ocean based on laser direct infrared imaging and microwave-assisted matrix digestion. Environ Pollut 307, 119547.
[24] da Costa Filho, P.A., Cobuccio, L., Mainali, D., Rault, M., Cavin, C., 2020. Rapid analysis of food raw materials adulteration using laser direct infrared spectroscopy and imaging. Food Control 113, 107114.
[25] Scircle, A., Cizdziel, J.V., Tisinger, L., Anumol, T., Robey, D., 2020. Occurrence of microplastic pollution at oyster reefs and other coastal sites in the Mississippi Sound, USA: impacts of freshwater inflows from flooding. Toxics 8 (2).
[26] Kotulanová, E., Bezdička, P., Hradil, D., Hradilová, J., Švarcová, S., Grygar, T., 2009. Degradation of lead-based pigments by salt solutions. J Cult Herit 10 (3), 367–378.
[27] Fremout, W., Saverwyns, S., 2012. Identification of synthetic organic pigments: the role of a comprehensive digital Raman spectral library. J Raman Spectrosc 43 (11), 1536–1544.
[28] Caggiani, M.C., Cosentino, A., Mangone, A., 2016. Pigments Checker version 3.0, a handy set for conservation scientists: a free online Raman spectra database. Microchem J 129, 123–132.
[29] Liland, K.H., Almøy, T., Mevik, B.-H., 2010. Optimal choice of baseline correction for multivariate calibration of spectra. Appl Spectrosc 64 (9), 1007–1016.
[30] Lieber, C.A., Mahadevan-Jansen, A., 2003. Automated method for subtraction of fluorescence from biological Raman spectra. Appl Spectrosc 57 (11), 1363–1367.

[31] Primpke, S., Cross, R.K., Mintenig, S.M., Simon, M., Vianello, A., Gerdts, G., et al., 2020. Toward the systematic identification of microplastics in the environment: evaluation of a new independent software tool (siMPle) for spectroscopic analysis. Appl Spectrosc 74 (9), 1127–1138.
[32] Primpke, S., Lorenz, C., Rascher-Friesenhausen, R., Gerdts, G., 2017. An automated approach for microplastics analysis using focal plane array (FPA) FTIR microscopy and image analysis. Anal Methods 9 (9), 1499–1511.
[33] Primpke, S., Wirth, M., Lorenz, C., Gerdts, G., 2018. Reference database design for the automated analysis of microplastic samples based on Fourier transform infrared (FTIR) spectroscopy. Anal Bioanal Chem 410.
[34] Bergmann, M., Wirzberger, V., Krumpen, T., Lorenz, C., Primpke, S., Tekman, M.B., et al., 2017. High quantities of microplastic in arctic deep-sea sediments from the HAUSGARTEN observatory. Environ Sci Technol 51 (19), 11000–11010.
[35] Lorenz, C., Roscher, L., Meyer, M.S., Hildebrandt, L., Prume, J., Löder, M.G.J., et al., 2019. Spatial distribution of microplastics in sediments and surface waters of the southern North Sea. Environ Pollut 252, 1719–1729.
[36] Imhof, H.K., Laforsch, C., Wiesheu, A.C., Schmid, J., Anger, P.M., Niessner, R., et al., 2016. Pigments and plastic in limnetic ecosystems: a qualitative and quantitative study on microparticles of different size classes. Water Res 98, 64–74.
[37] Catrouillet, C., Davranche, M., Khatib, I., Fauny, C., Wahl, A., Gigault, J., 2021. Metals in microplastics: determining which are additive, adsorbed, and bioavailable. Environ Sci Process Impacts 23 (4), 553–558.
[38] Gharbi, O., Thomas, S., Smith, C., Birbilis, N., 2018. Chromate replacement: what does the future hold? npj Mater Degrad 2 (1), 12.
[39] Shams El Din, A.M., Wang, L., 1996. Mechanism of corrosion inhibition by sodium molybdate. Desalination 107 (1), 29–43.
[40] Deepa, M.J., Arunima, S.R., Shibli, S.M.A., 2022. Hydrophobic and corrosion-resistant composite (BiVO4/TiO2) hot-dip zinc coating with enhanced self-cleaning ability. J Alloy Compd 924, 166522.
[41] Turner, A., Filella, M., 2021. Hazardous metal additives in plastics and their environmental impacts. Environ Int 156, 106622.
[42] Kopylov, N.I., Kaplin, Y.M., Litvinov, V.P., Kaminskii, Y.D., 2007. Large-scale use of arsenic in the production of antifouling coatings. Theor Found Chem Eng 41 (5), 780–785.
[43] Gázquez, M.J., Moreno, S.M.P., Bolívar, J.P., 2021. 9 - TiO2 as white pigment and valorization of the waste coming from its production. In: Parrino, F., Palmisano, L. (Eds.), Titanium dioxide (Tio_2) and its applications. Elsevier, pp. 311–335.
[44] Faure B, Salazar-Alvarez G, Ahniyaz A, Villaluenga I, Berriozabal G, De Miguel YR, et al. Dispersion and surface functionalization of oxide nanoparticles for transparent photocatalytic and UV-protecting coatings and sunscreens; 2013. p.1468–6996 (Print).
[45] Baan, R., K. Straif, Y. Grosse, B. Secretan, F. El Ghissassi , V. Cogliano2006. Carcinogenicity of carbon black, titanium dioxide, and talc. p. 1470–2045 (Print)).
[46] Dar, G.I., M. Saeed , A. Wu2020. Toxicity of TiO2 nanoparticles. TiO2 nanoparticles. p. 67–103.
[47] Tamburini, D., 2021. Analytical pyrolysis applied to the characterisation and identification of Asian lacquers in cultural heritage samples – a review. J Anal Appl Pyrolysis 157, 105202.
[48] Pellis, G., Bertasa, M., Ricci, C., Scarcella, A., Croveri, P., Poli, T., Scalarone, D., 2022. A multi-analytical approach for precise identification of alkyd spray paints and for a better understanding of their ageing behaviour in graffiti and urban artworks. J Anal Appl Pyrolysis 165, 105576.
[49] Godwin, A.D., 2017. In: Kutz, M. (Ed.), 24 - Plasticizers. applied plastics engineering handbook, second edition. William Andrew Publishing.
[50] Richter, D., Massmann, G., Dünnbier, U., 2008. Identification and significance of sulphonamides (p-TSA, o-TSA, BSA) in an urban water cycle (Berlin, Germany). Water Res 42 (6), 1369–1378.